Briefing Space Weather - 2022/04/25

Sun

Responsible: José Cecatto

04/18 – Fast (=< 600 km/s) wind stream; 6 CME c.h.c. toward the Earth;
04/19 – Fast (=< 550 km/s) wind stream; 4 CME c.h.c. toward the Earth – 1 partial halo;
04/20 – Fast (=< 500 km/s) wind stream; 6 CME c.h.c. toward the Earth; ass X2.2, type-II / CME & radio blackout;
04/21 – Fast (=< 450 km/s) wind stream; 7 CME c.h.c. toward the Earth; ass M9.6, type-II / CME & radio blackout;
04/22 – Fast (=< 500 km/s) wind stream; 1 CME c.h.c. toward the Earth;
04/23 – Fast (=< 500 km/s) wind stream; 4 CME c.h.c. toward the Earth;
04/24 – Fast (=< 500 km/s) wind stream; 4 CME c.h.c. toward the Earth – 1 partial halo;
04/25 – Fast (=< 450 km/s) wind stream; 2 CME c.h.c. toward the Earth;
Prev.: Fast wind expected on April 29; for while good (40% M, 10% X) probability of M / X flares next 2 days; also, occasionally other CME can present component toward the Earth. c.h.c. – can have a component

Responsible: Douglas Silva

WSA-ENLIL (CME 2022-04-21T02:36Z)
● The simulation results indicate that the flank of CME will reach the DSCOVR mission between
2022-04-24T17:00Z and 2022-04-25T07:00Z.

Coronal holes (SPOCA):

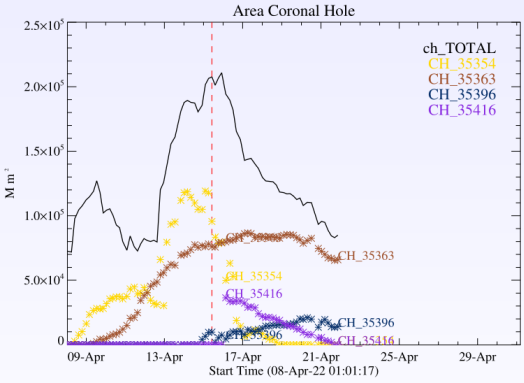

Figura: The solid line in black shows the products of the sum of areas for each detection interval performed by SPOCA between April 8th and 24th, 2022.

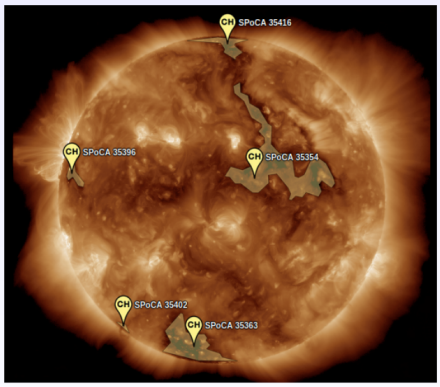

Figura: Above the 193 Å image of the Sun are highlighted coronal holes observed by SPOCA around 12:00 UT on April 16, 2022.

WSA - ENLIL SPOCA

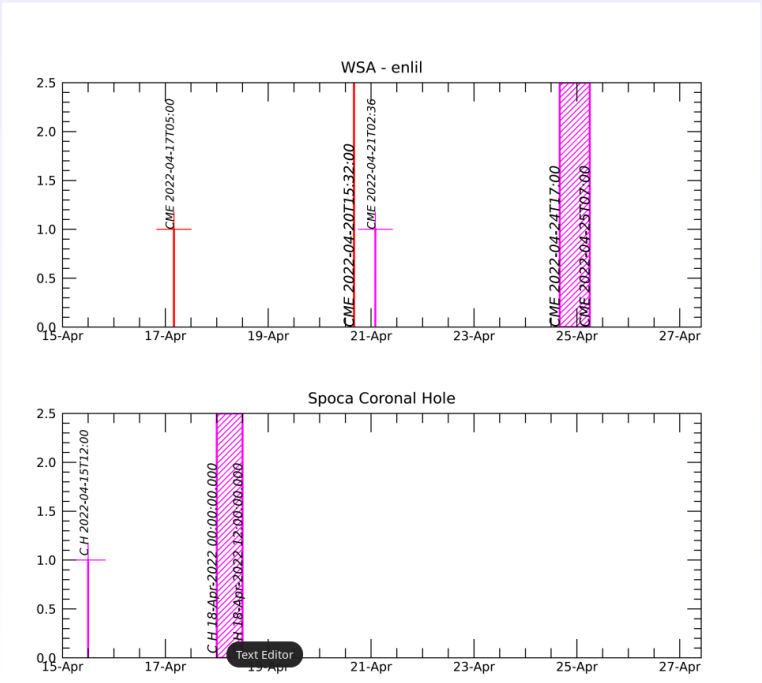

Responsible: Paulo Ricardo Jauer

Resumo dos índices do meio interplanetário

Máximos diários - mais recentes entre 18 Abr, 2022 e 25 Abr, 2022

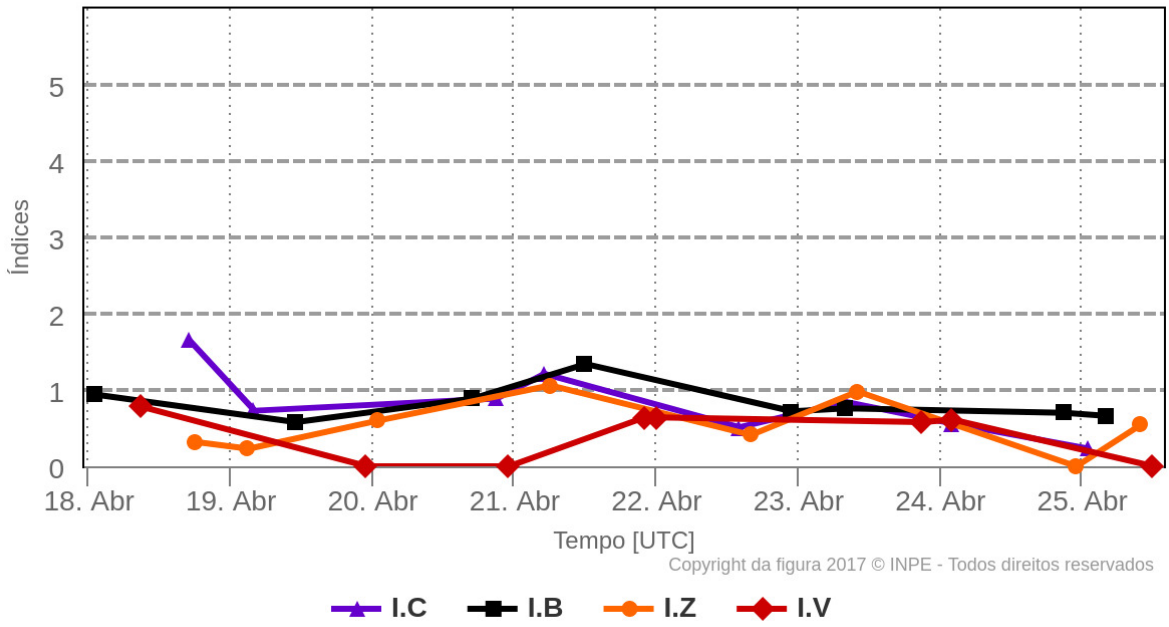

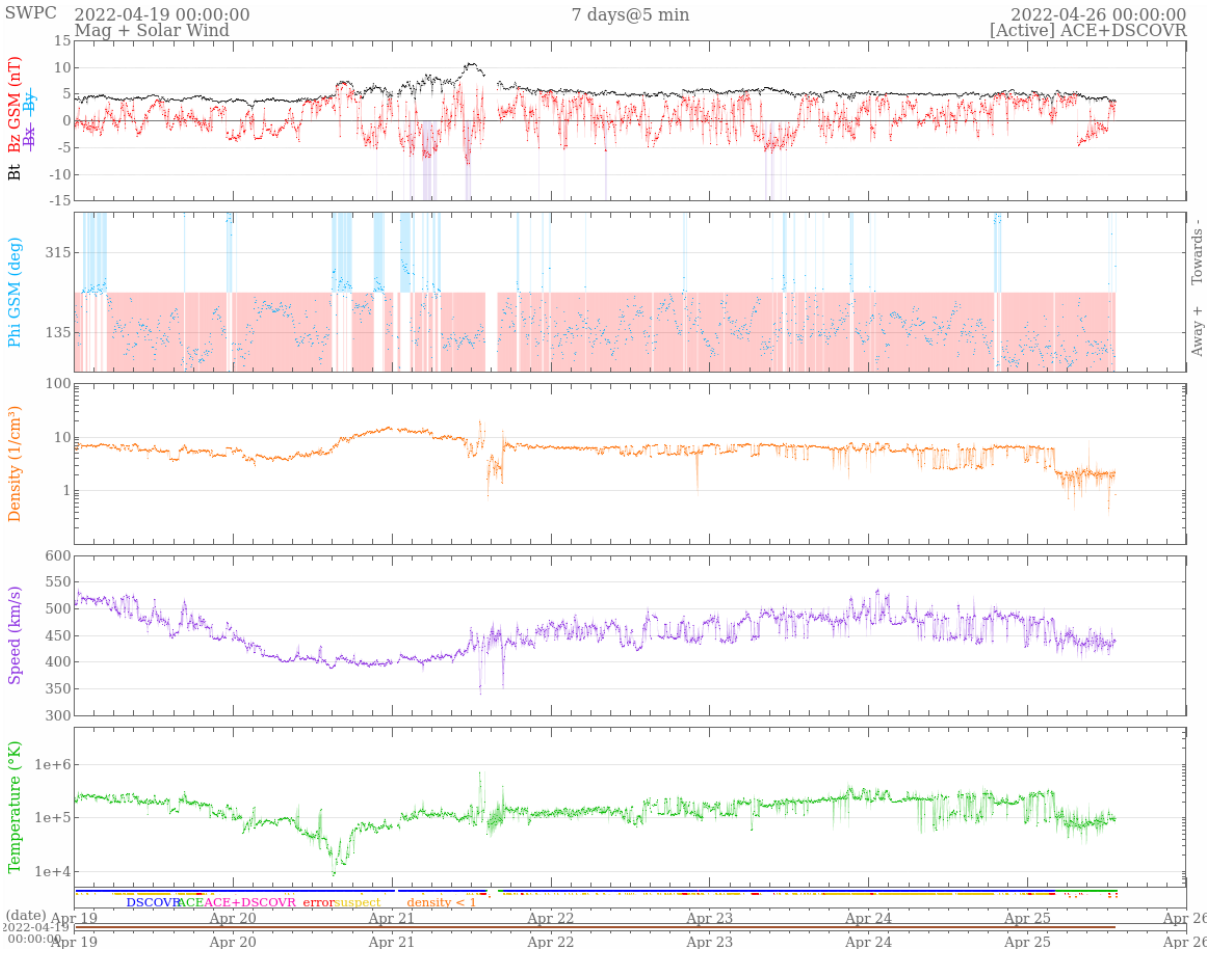

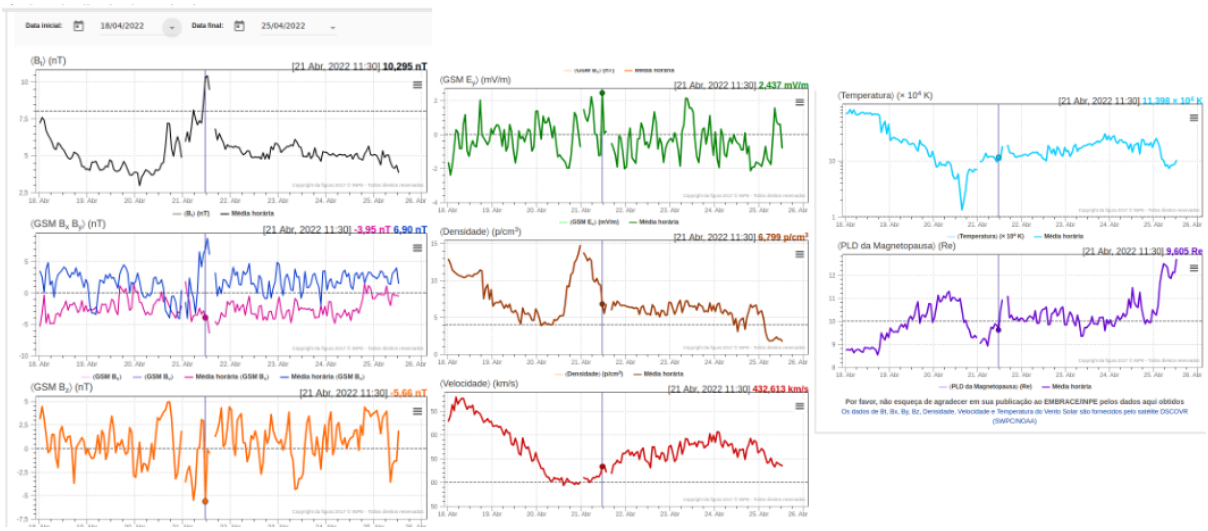

- The interplanetary region in the last week showed a moderate of plasma perturbations due to the passage of the CME and HSS structures identified by the DISCOVERY satellite in the interplanetary region.
- The modulus of the component of the interplanetary magnetic field showed 1 maximum peak : 21/Apr at 13:30 of ~ 9.48 nT.
- The BxBy components showed intense variations in the analyzed period, due to the characteristic of magnetic cloud and HSS, it becomes a complex event. The by component showed a maximum peak on Apr/21 at 12:30 8.6 nT.
- The component of the bz field showed fluctuations due to the interplanetary structure of the Magnetic Cloud type, however, due to the interaction with Hss, it becomes a complex structure. The minimum value presented in the bz component was -5.66 nT on Apr/21 at 11:30 UT. Conditions favorable to the emergence of geomagnetic disturbances
- The solar wind density showed a maximum peak on 20/Apr at 23:30 UT of 14.7 p/cm³. However, the density presented variations before and after this maximum peak due to the interaction of the fast solar wind and CME.
- The solar wind speed had oscillated mostly above 400 km/s throughout the presenting period. It presented a minimum value on 20/Apr at 20:30 of 395km/s, it also presented a maximum value of 578 km/s at 04:30 on 18/Apr.
- The magnetopause position was oscillating on average around the typical 10 Re position. The maximum compression was observed on 18/Apr at 17:30 UT of 8.5 Re.

Radiation Belts

Responsible: Ligia Alves Da Silva

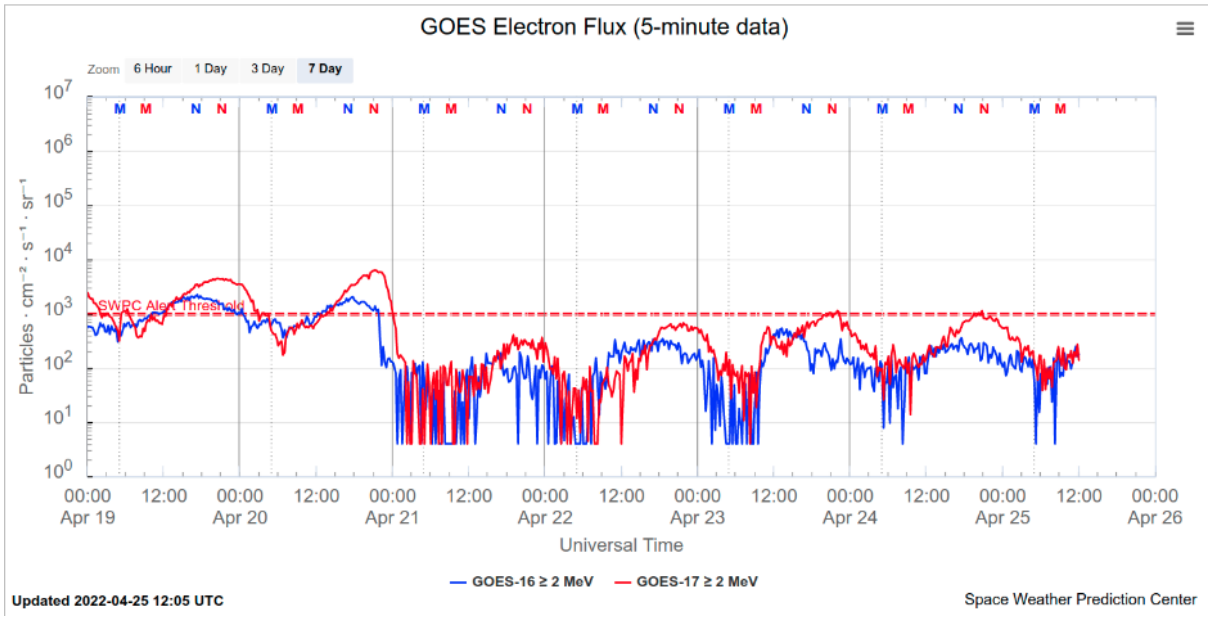

Figure 1: High-energy electron flux (> 2MeV) obtained from GOES-16 and GOES-17 satellite. Source: https://www.swpc.noaa.gov/products/goes-electron-flux

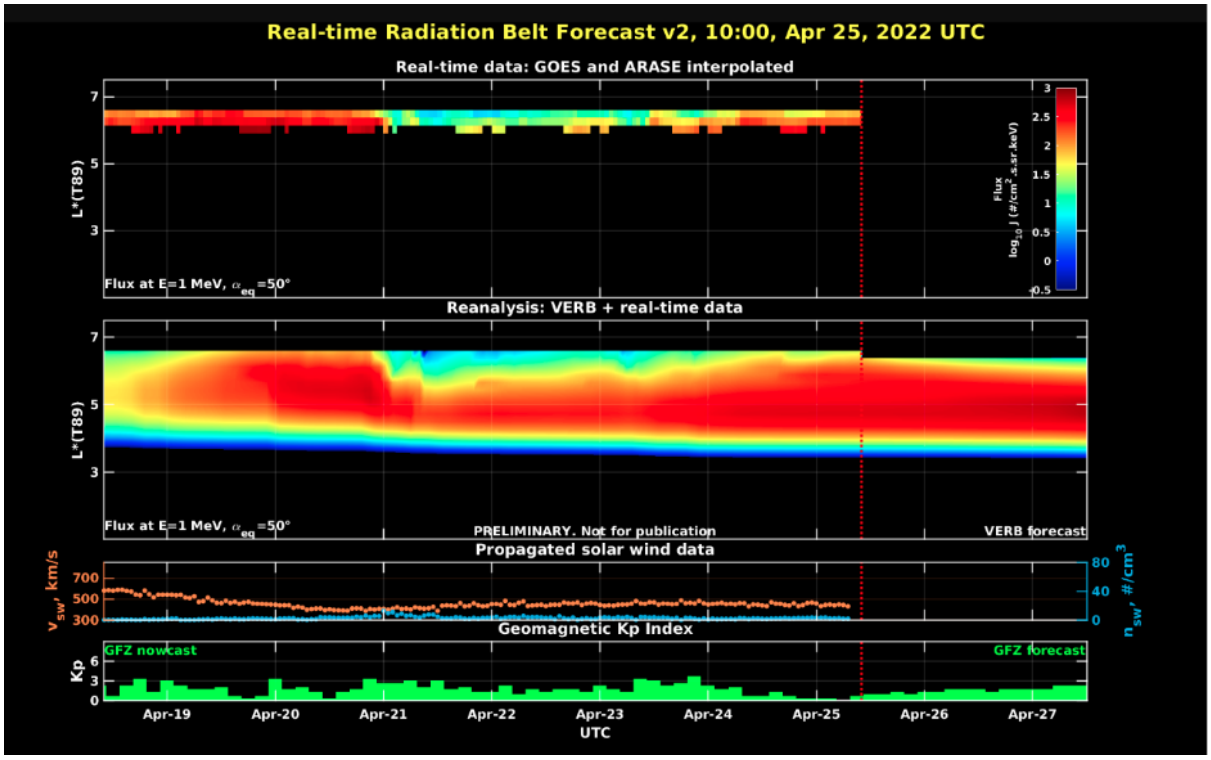

Figure 2: high-energy electron flux data (real-time and interpolated) obtained from ARASE, GOES-16, GOES-17
satellites. Reanalysis's data from VERB code and interpolated electron flux. Solar wind velocity and proton density data from ACE satellite. Source: https://rbm.epss.ucla.edu/realtime-forecast/

High-energy electron flux (>2 MeV) in the outer boundary of the outer radiation belt obtained from geostationary satellite data GOES-16 and GOES-17 (Figure 1) is oscillating around the minimum threshold (103 particles/(cm2 s sr)) on April 19-20th. An electron flux decrease of approximately 2 orders of magnitude starts at the end of April 20th, persisting below 103 particles/(cm2 s sr) until today, April 25th. However, it is essential to highlight that the electron flux is above 102 particles/(cm2 s sr) on average from 15:00 Z on April 22nd.

The GOES-16, GOES-17, and Arase satellite data are analyzed and interpolated to observe the high-energy electron flux variability (1 MeV) in the outer radiation belt (Figure 2). Additionally, the VERB code rebuilds this electron considering the Ultra Low Frequency (ULF) waves' radial diffusion. The simulation (VERB code) shows that the electron flux decrease observed from April 20th reached L-shell = 5.0 on April 21st. This electron flux variability occurred concomitantly with the arrival of the coronal mass ejections and ULF wave activities. However, it is important to point out that the data from the ARASE satellite are not available for the week under analysis to confirm
the L-shell level of this referred electron flux decrease.

ULF waves in the Magnetosphere

Responsible: José Paulo Marchezi

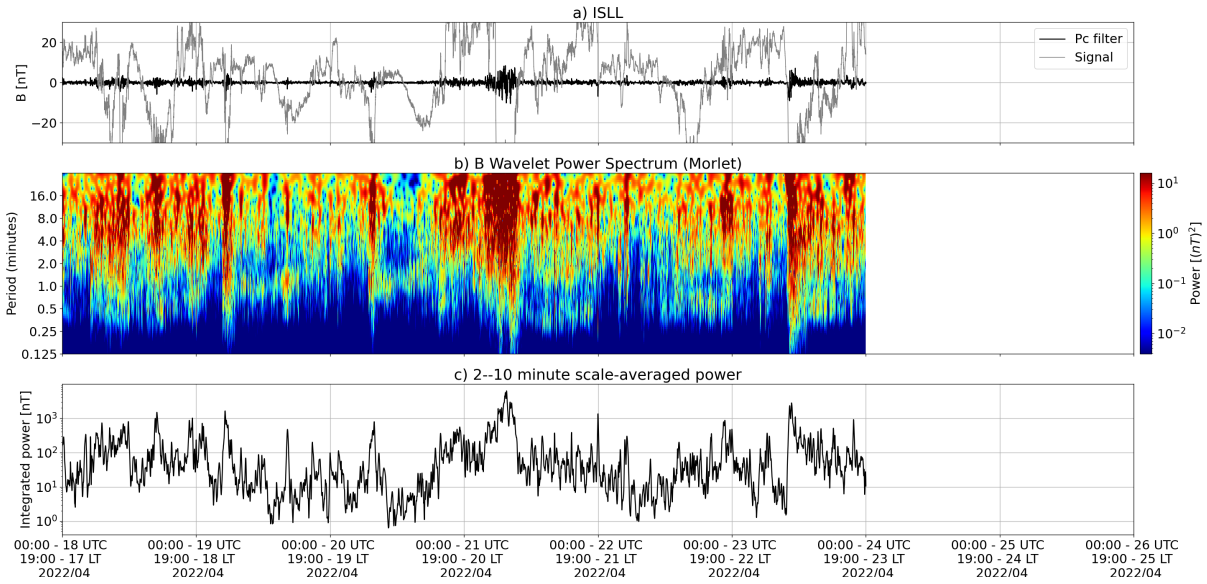

a) signal of the total magnetic field measured in the ISLL Station of the CARISMA network in gray, together with the fluctuation in the range of Pc5 in black. b) Wavelet power spectrum of the filtered signal. c) Average spectral power in the ranges from 2 to 10 minutes (ULF waves).

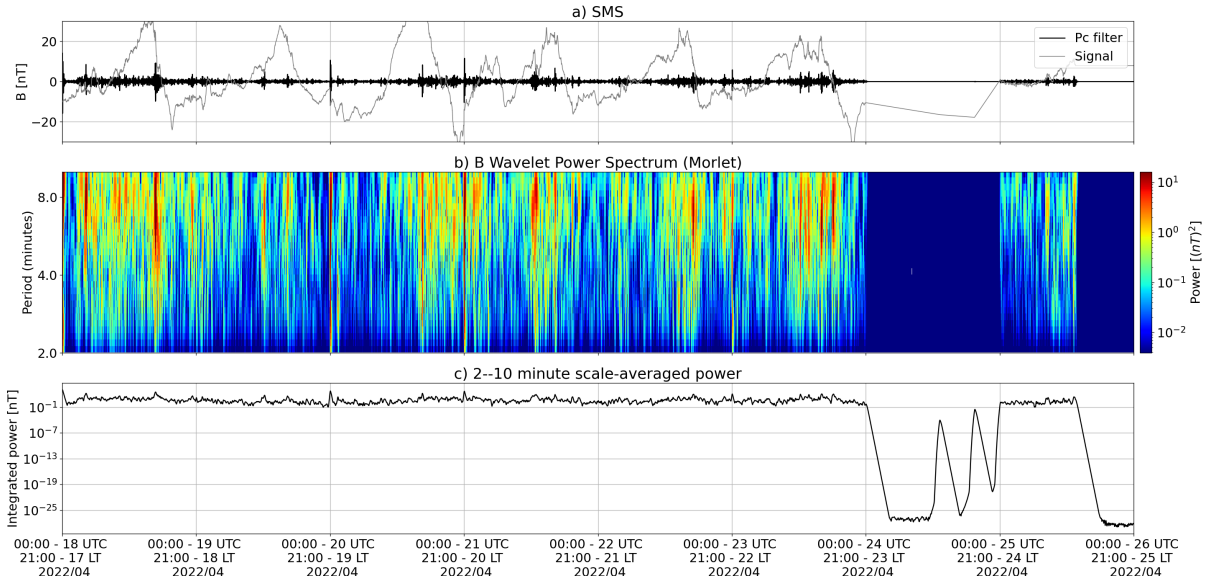

a) signal of the total magnetic field measured in the SMS Station of the EMBRACE network in gray, together with the fluctuation in the range of Pc5 in black. b) Wavelet power spectrum of the filtered signal. c) Average spectral power in the ranges from 2 to 10 minutes (ULF waves).

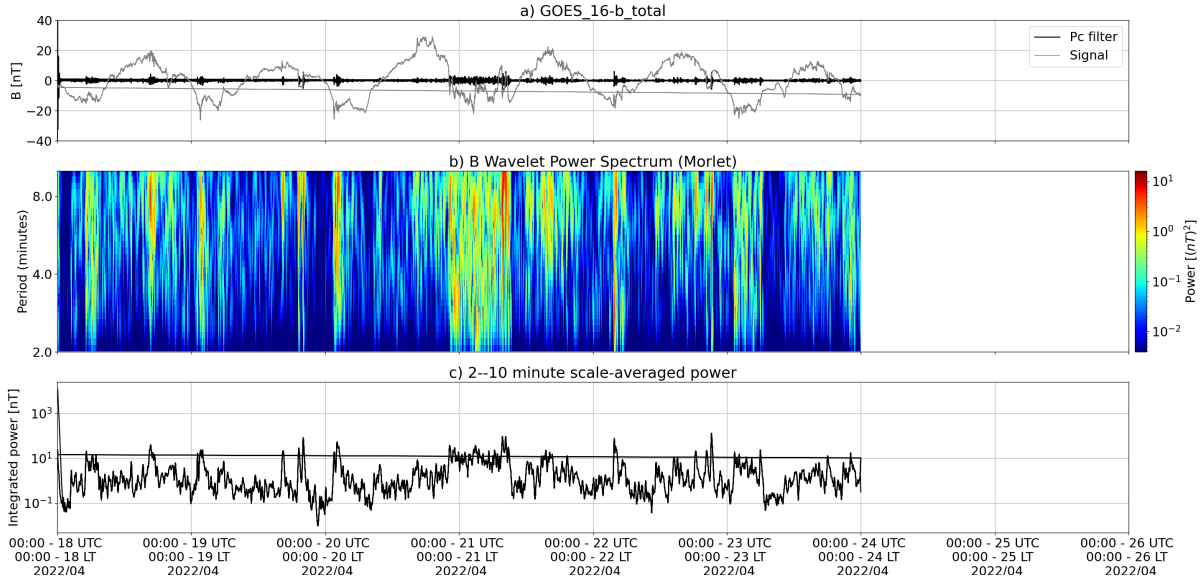

a) signal of the total magnetic field measured by the GOES 16 satellite, together with the fluctuation in the range of Pc5 in black. b) Wavelet power spectrum of the filtered signal. c) Average spectral power in the ranges from 2 to 10 minutes (ULF waves).

The ULF wave activity shows an increase in power from the 18th of April in the form of continuous pulsations, detected from high latitudes to the magnetometers at low latitudes of the EMBRACE network (Figure 2, SMS). On the 21st and 22nd of April, new increases in ULF power are observed at high latitudes and with an impulsive characteristic on the 22nd, with fluctuations remaining until the 23rd of April, when there is a new abrupt variation in the spectral power, mainly at high latitudes. and also detected by the GOES satellite, possibly associated with the interaction of a CME followed by an HSS.

EMIC waves in the Magnetosphere

Responsible: Claudia Medeiros

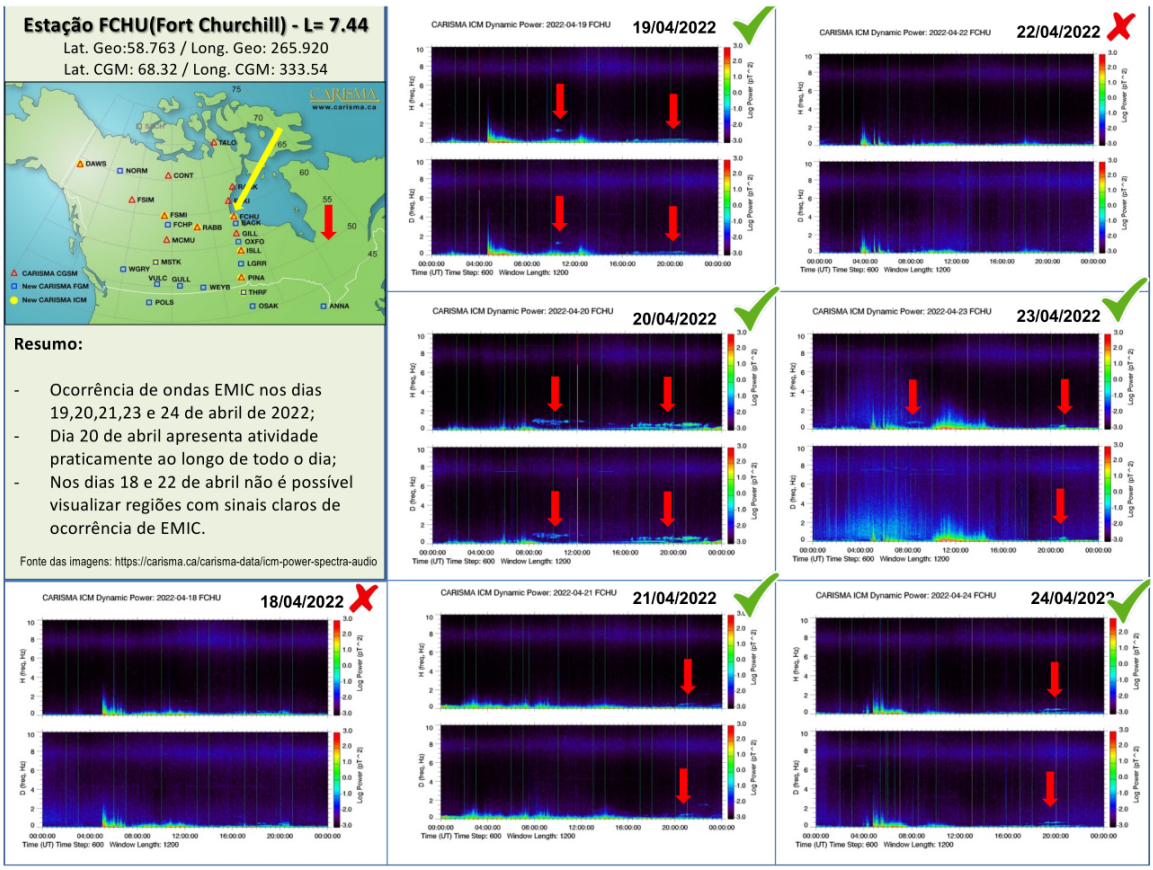

Geomagnetism

Responsible: Livia Ribeiro Alves

Ionosphere

Responsible: Laysa Resende

Boa Vista:

- There were spread F during all days in this week.
- The Es layers reached scale 3 on days 19 and 23.

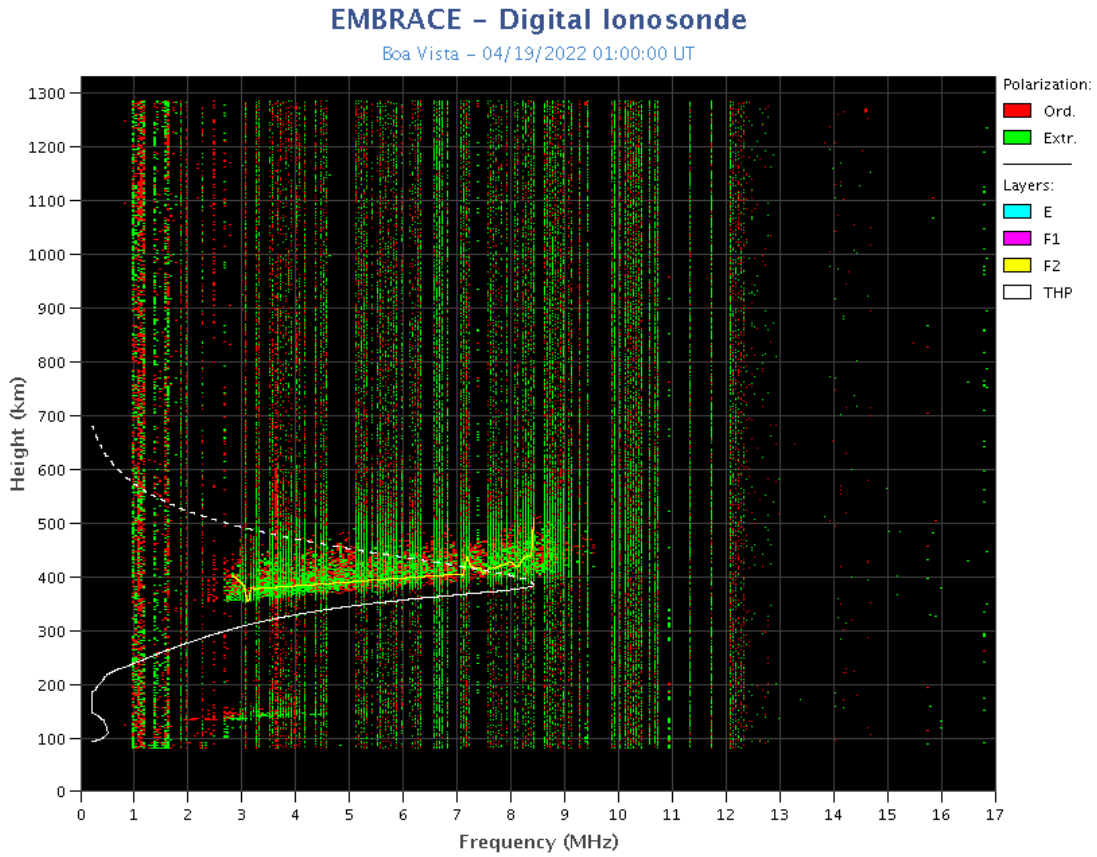

Cachoeira Paulista:

- There were not spread F in this week.
- The Es layers reached scale 3 on day 19.

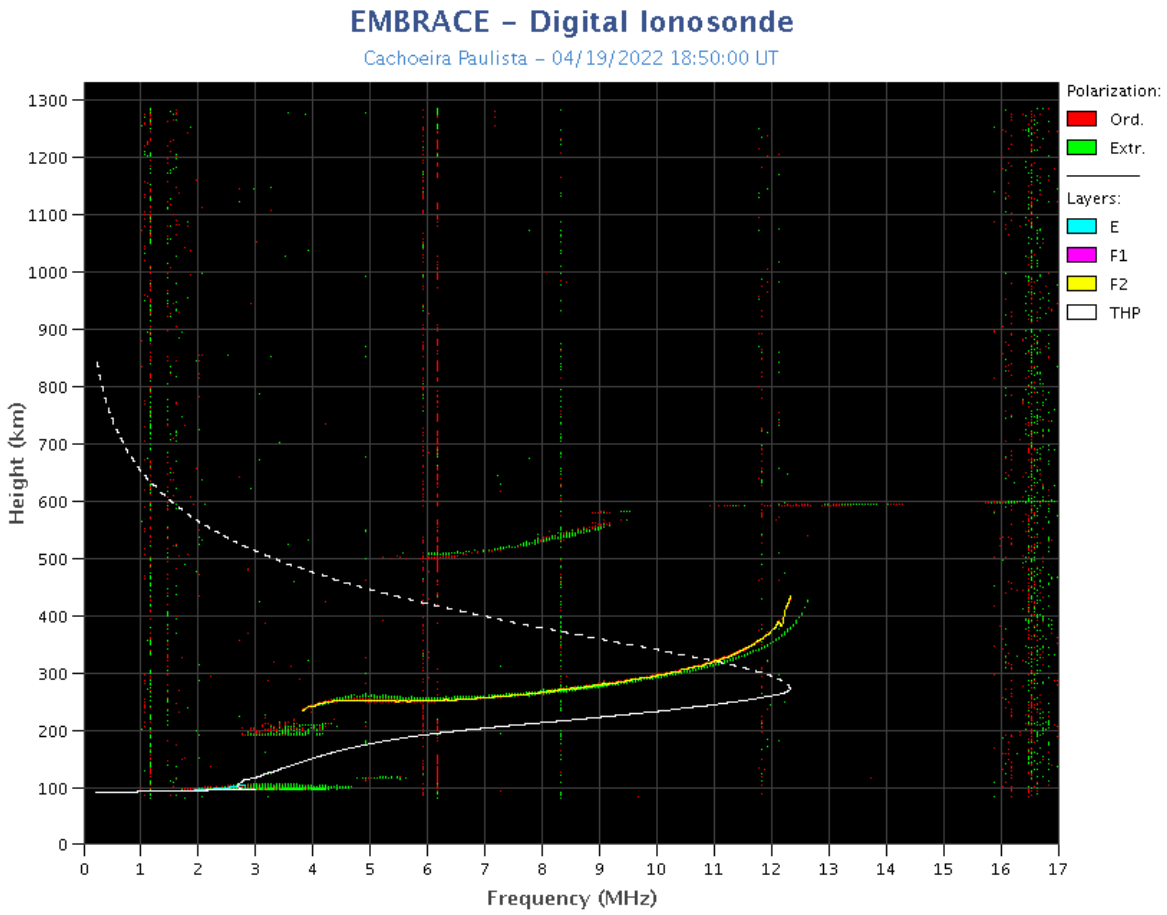

São Luís:

- There were spread F during all days in this week.
- The Es layers reached scale 5 on day 21.

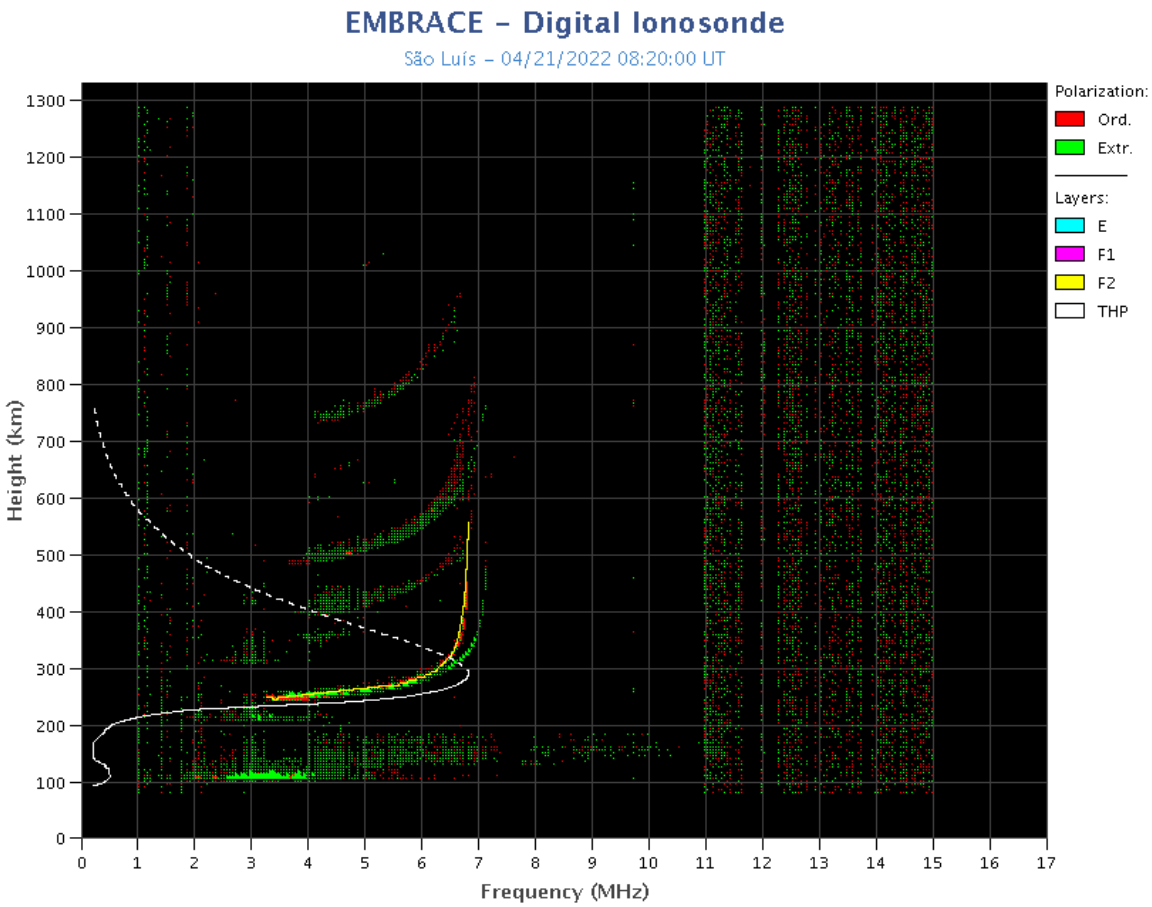

Scintillation S4

Responsible: Siomel Savio Odriozola

In this report on the S4 scintillation index, data from SLMA in São Luiz/MA, STSN in Sinop/MT, UFBA, in Bahía/BA and SJCE in São José dos Campos/SP are presented. The S4 index tracks the presence of irregularities in the ionosphere having a spatial scale ~ 360 m.

Weak values of the S4 index (~0.3—0.4) were measured after dusk only at the SLMA station on 18 /04 (Figure 1). The rest of the stations did not show S4 above 0.3 which confirms the end of the bubble season in Brazil.

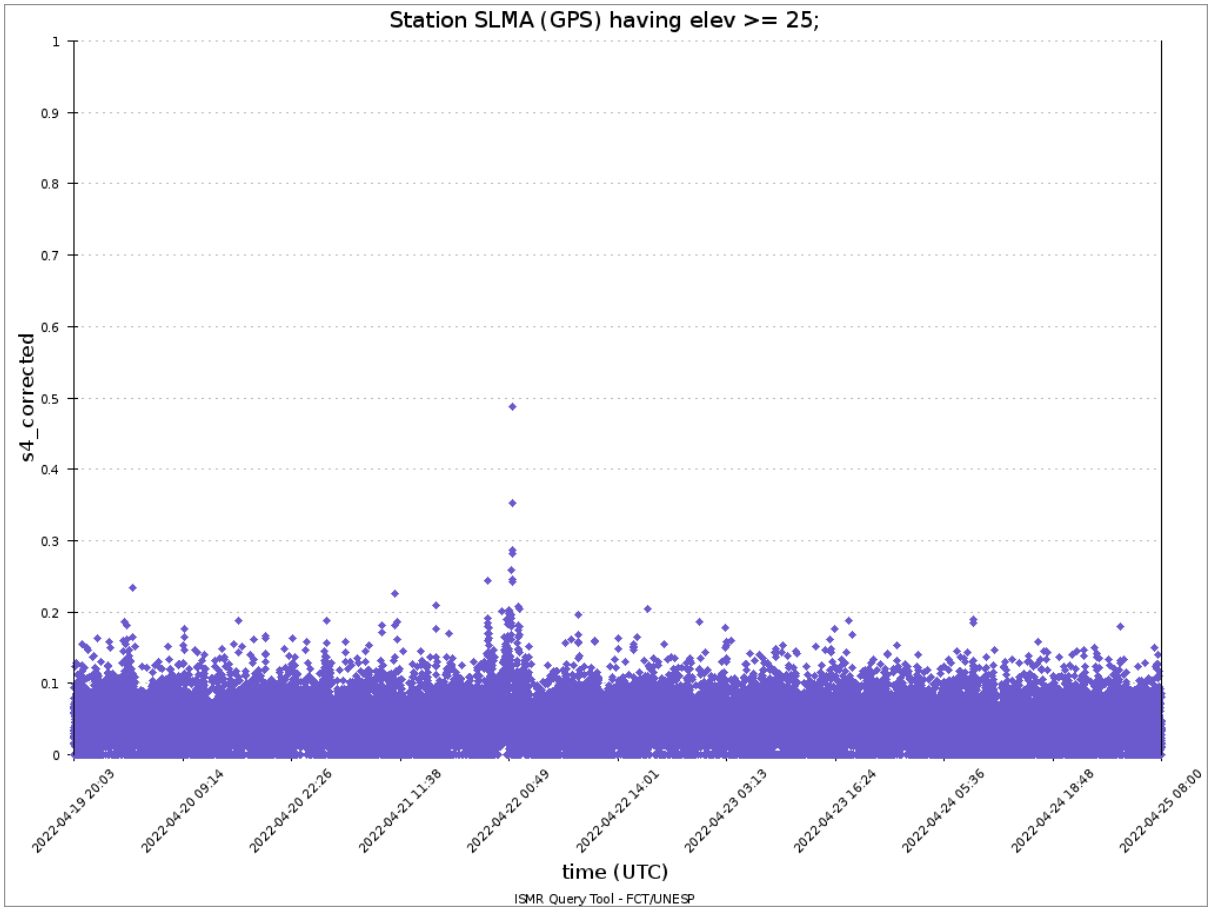

Figure 1: S4 index values corresponding to the GPS constellation measured at SLMA during the week 04/ 18-25.

All-Sky Imager

Responsible: Cosme Alexandre

ROTI

Responsible: Carolina de Sousa do Carmo

The ROTI (Rate of TEC index) is an index based on the variation of the TEC (Total Electron Content) (Pi et al., 1997). This index is used to detect ionospheric irregularities, such as plasma bubbles. The ROTI index shows a good correlation with the S4 scintillation index (e.g., Carrano
et al., 2019). **Table 1** shows the week's summary (April 17-23, 2022) according to the ROTI

index, showing the times of detection of ionospheric irregularities in the South American sector. In addition, Figures 1 shows the keograms of the ROTI index, for fixed geographic latitudes 5°S and
15°S, with geographic longitude versus universal time (UT).

Week	Day	Time of occurrence (UT)
Sunday	2022/04/17	-
Monday	2022/04/18	-
Tuesday	2022/04/19	-
Wednesday	2022/04/20	22:00-24:00
Thursday	2022/04/21	No data
Friday	2022/04/22	No data
Saturday	2022/04/23	No data

Table 1 – Weekly Summary (April 17-23, 2022).

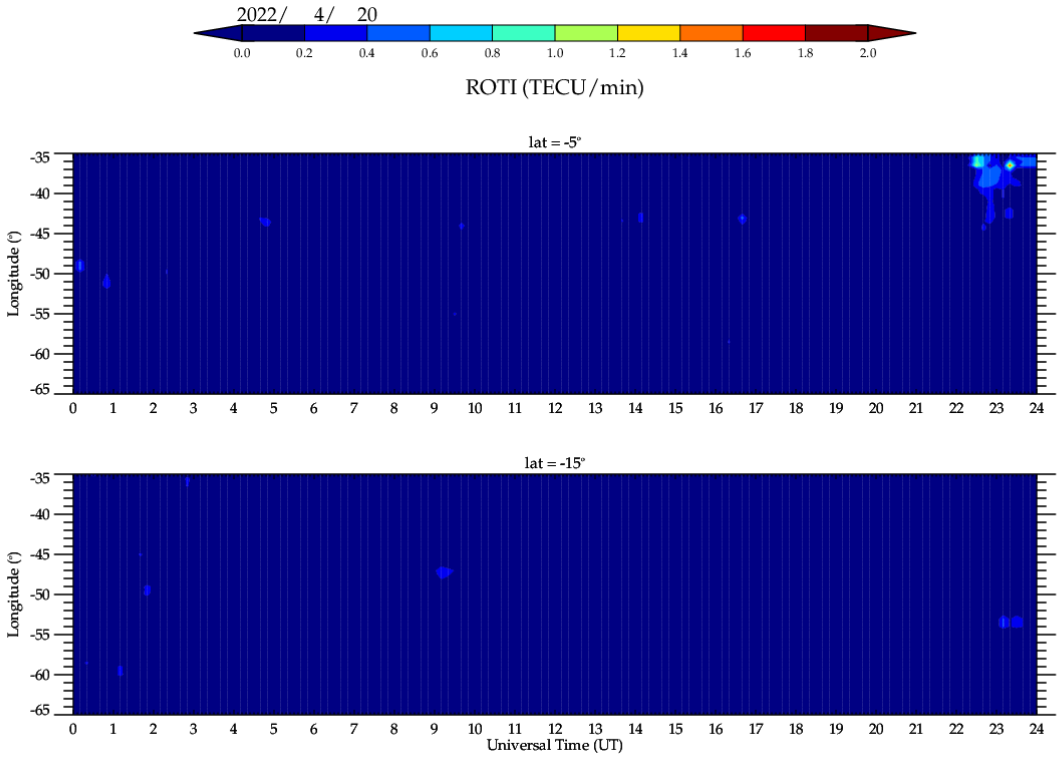

Figure 1 - Keogram of the ROTI index for fixed geographic latitudes 5°S and 15°S, on April 20, 2022.